

# The Interaction of Radio Sources and X-Ray-Emitting Gas in Cooling Flows

Elizabeth L. Blanton<sup>1,2</sup>

<sup>1</sup> *University of Virginia, Department of Astronomy, P.O. Box 3818, Charlottesville, VA 22903; eblanton@virginia.edu*

<sup>2</sup> *Chandra Fellow*

Recent observations of the interactions between radio sources and the X-ray-emitting gas in cooling flows in the cores of clusters of galaxies are reviewed. The radio sources inflate bubbles in the X-ray gas, which then rise buoyantly outward in the clusters transporting energy to the intracluster medium (ICM). The bright rims of gas around the radio bubbles are cool, rather than hot, and do not show signs of being strongly shocked. Energy deposited into the ICM over the lifetime of a cluster through several outbursts of a radio source helps to account for at least some of the gas that is missing in cooling flows at low temperatures.

## 1. Introduction

The vast majority of cooling flow clusters contain powerful radio sources associated with central cD galaxies. Initial evidence of radio sources displacing, and evacuating cavities in, the X-ray-emitting intracluster medium (ICM) was found with *ROSAT* observations of a few sources including Perseus (Böhringer et al. 1993), Abell 4059 (Huang & Sarazin 1998), and Abell 2052 (Rizza et al. 2000). Models predicted that the radio sources would shock the ICM, and that the X-ray emission surrounding the lobes would appear hot (Heinz, Reynolds, & Begelman 1998). High-resolution images from *Chandra* have revealed many more cases of radio sources profoundly effecting the ICM by displacing it and creating X-ray deficient “holes” or “bubbles.” The *Chandra* data allow us to study the physics of the interaction in much more detail (e.g. Hydra A, McNamara et al. 2000; Perseus, Fabian et al. 2000; Abell 2052, Blanton et al. 2001; Abell 2597, McNamara et al. 2001; Abell 496, Dupke & White, 2001; MKW 3s, Mazzotta et al. 2002; RBS797, Schindler et al. 2001; Abell 2199, Johnstone et al. 2002; Abell 4059, Heinz et al. 2002; Virgo, Young et al. 2002; Centaurus, Sanders & Fabian 2002; Cygnus A, Smith et al. 2002; Abell 478, Sun et al. 2003).

A long-standing problem with cooling flow models has been that the mass of gas measured to be cooling from X-ray temperatures, based on surface-brightness and spectral studies with *Einstein* and *ROSAT* has not been detected in sufficient quantities at cooler temperatures. High-resolution spectroscopy with *XMM-Newton* provided direct evidence that gas was cooling in these clusters, but very large masses of gas (hundreds of solar masses) were seemingly cooling over only a limited range of temperatures. Emission lines such as Fe XVII expected from gas cooling below approximately 2 keV were not detected and in general, most of the ICM seems to cool to about one-half to one-third of the cluster ambient temperature (Peterson et al. 2003). Several possible solutions have been proposed for the lack of cool X-ray gas seen in the new observations (Fabian et al. 2001;

Peterson et al. 2001). These include mixing, heating by central active galactic nuclei (AGN), inhomogeneous abundances, and differential absorption. Heating of the gas by a central radio source has also been discussed recently by Böhringer et al. (2002), Churazov et al. (2002), Ruszkowski & Begelman (2002), Kaiser & Binney (2003), and Brüggén (2003), among others.

A common finding with the *Chandra* data is X-ray deficient holes that correspond with radio emission from the lobes of a central AGN. These holes are typically surrounded by bright shells of dense, X-ray-emitting gas. One of the surprises of the *Chandra* observations is that the X-ray-bright rims surrounding the radio sources observed in cooling flow clusters were found to be cooler, rather than hotter, than the neighboring cluster gas (e.g. Perseus, Schmidt et al. 2002; Hydra A, Nulsen et al. 2002; Abell 2052, Blanton et al. 2003). The bright shells show no evidence of current strong shocks. Soker, Blanton, & Sarazin (2002) found that for the case of Abell 2052, the morphology was well-explained by weak shocks occurring in the past, and strong shocks were generally ruled out. To date, no case of current strong-shock heating of the ICM in a cooling flow cluster by an AGN has been observed. Although strong-shock heating from the radio source as proposed by Heinz, Reynolds, & Begelman (1998) and Rizza et al. (2000) may not be the explanation for the fate of the missing cool gas, energy input from a radio source in the form of weak shocks (e.g. Reynolds, Heinz, & Begelman 2002) and buoyantly rising bubbles of relativistic plasma (e.g. Churazov et al. 2002) can still contribute to heating.

## 2. *Chandra* Observations of Bubbles and Temperature Structure

The first cooling flow cluster with a central radio source observed by *Chandra* was Hydra A (McNamara et al. 2000; David et al. 2001, Nulsen et al. 2002). Hydra A is a powerful, doubled-lobed, FR I radio source (3C 218), and the radio lobes were found to be anti-correlated with the cluster gas. The cavities evacuated by the radio source

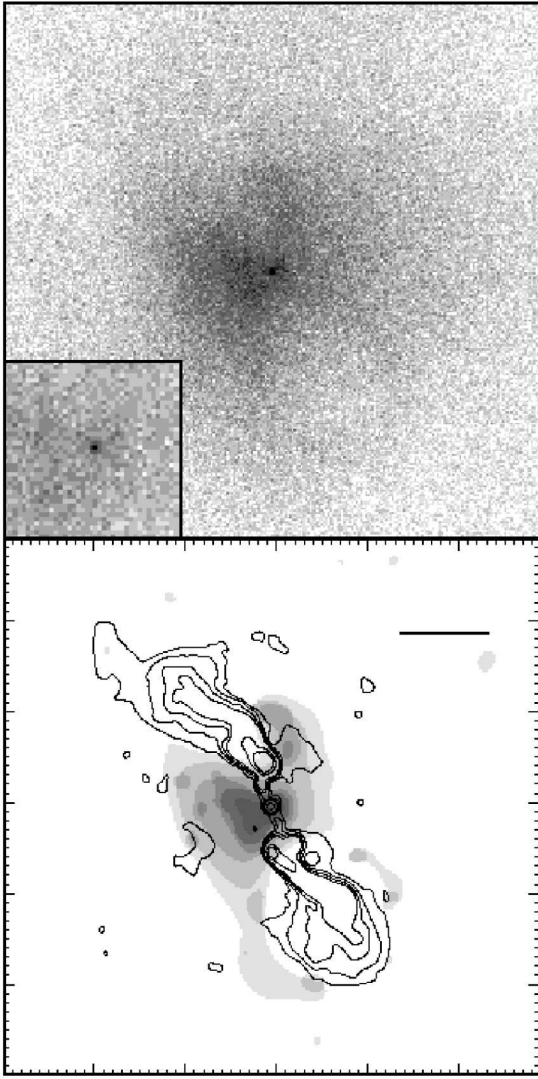


FIG. 1.— The first radio source / cluster cooling flow interaction observed with *Chandra*: Hydra A (McNamara et al. 2000).

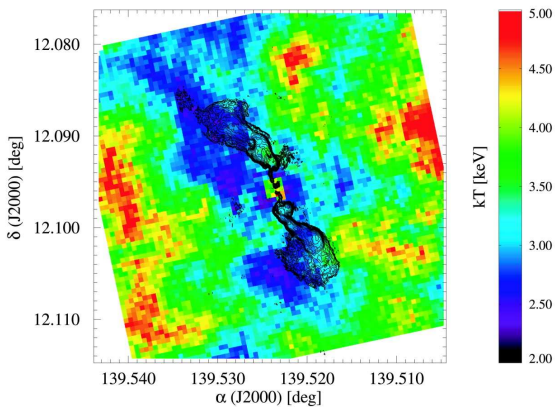


FIG. 2.— The temperature map of the Hydra A cluster, with radio contours superposed (Nulsen et al. 2002). The coolest gas is found in the regions surrounding the radio source, and there is no evidence for current strong-shock heating of the ICM from the radio lobes.

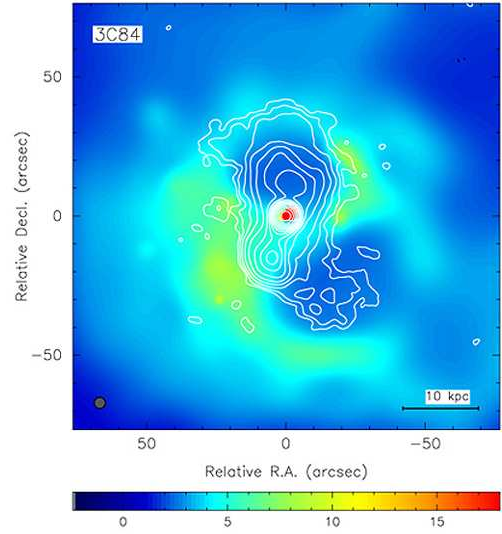


FIG. 3.— Overlay of radio contours onto the adaptively-smoothed *Chandra* X-ray image of the Perseus cluster. Radio: NSF/AURA/VLA; X-ray: NASA/IOA/A. Fabian et al.

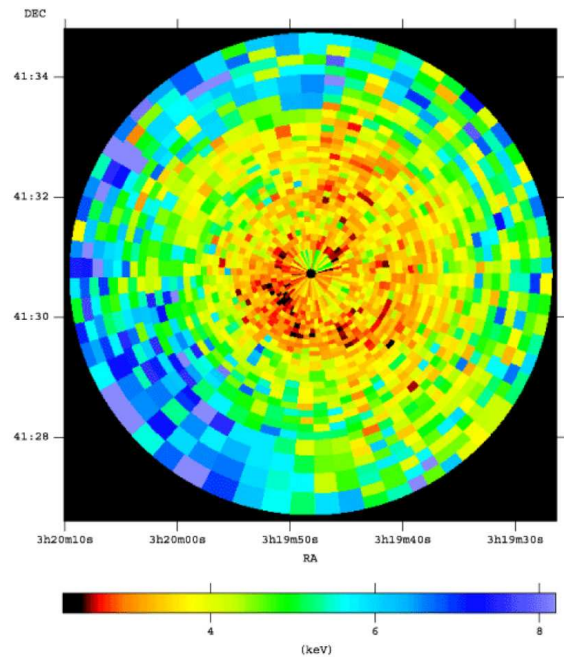


FIG. 4.— Temperature map of the central regions of the Perseus cluster (Schmidt et al. 2002).

are approximately 25 kpc in diameter. An image of the radio source / X-ray gas interaction is shown in Figure 1, and is from McNamara et al. (2000). The cooling time in the center of the cluster is  $6 \times 10^8$  yr, and surprisingly, the *coolest* gas was found in the regions surrounding the lobes. This is seen in the temperature map from Nulsen et al. (2002), shown here in Figure 2. There is currently no evidence that the radio source is strongly shocking the ICM, but weak shocks are not ruled out with a limit on the Mach number of  $\mathcal{M} < 1.23$ . The cooling of the ICM is found to occur only over a limited temperature range, and repeated outbursts from the ra-

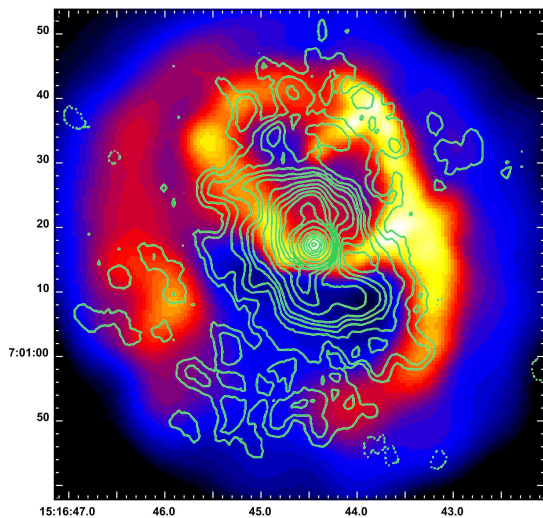


FIG. 5.— Overlay of 1.4 GHz radio contours onto the adaptively-smoothed *Chandra* image of Abell 2052 (Blanton et al. 2001, 2003).

radio source would be necessary to prevent cooling to lower temperatures (David et al. 2001).

The Perseus cluster (Abell 426) was first observed with *Chandra* in early 2000 (Fabian et al. 2000). This nearby cooling flow cluster ( $z = 0.0183$ ) is the brightest cluster in the X-ray sky and contains the powerful double-lobed radio source 3C 84 in the central galaxy, NGC 1275. Perseus provides one of the clearest examples of the interaction between the central radio source and the X-ray-emitting ICM, and signs of the interaction were already seen in the *ROSAT* data (Böhringer et al. 1993). The cluster exhibits two distinct bubbles in the X-ray gas that are filled with 1.4 GHz radio plasma and surrounded by bright shells of X-ray emission. The adaptively-smoothed *Chandra* image of the center of Perseus, with radio contours superposed, is shown in Figure 3 (Fabian et al. 2000). The cooling time in the cluster center is approximately  $10^8$  yr, and no evidence for current strong-shock heating is seen in the temperature map (Figure 4, Schmidt et al. 2002). The regions surrounding the radio source are the coolest in the X-ray. Presented at this meeting were initial exciting results from a much deeper observation of the Perseus cluster that was performed by *Chandra* in 2003, revealing intriguing ripple features in the X-ray surface brightness that are interpreted as resulting from the propagation of weak shocks and viscously-dissipating sound waves into the ICM and resulting from repeated outbursts of the central radio source (Fabian, this conference; Fabian et al. 2003).

Abell 2052 shows structures in its center that are very similar to those in Perseus. This cluster is nearby ( $z = 0.0348$ ), and the central cD galaxy is host to the powerful, double-lobed FR I radio source 3C 317. The *Chandra* image (Blanton et al. 2001, 2003) revealed clear deficits in the X-ray emission to the north and south of the cluster center that are filled with 1.4 GHz radio emission (Fig. 5). The bubbles are approximately 20 kpc in diameter and are surrounded by bright shells of X-ray

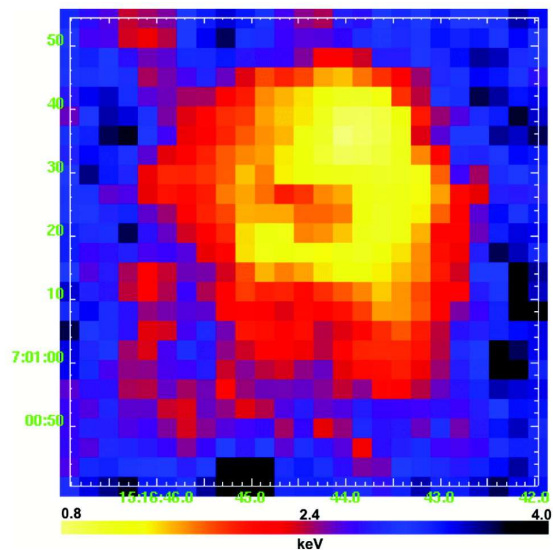


FIG. 6.— Temperature map of the central region of Abell 2052 derived from the *Chandra* data (Blanton et al. 2003). The shells surrounding the radio source are cool and show no signs of strong-shock heating.

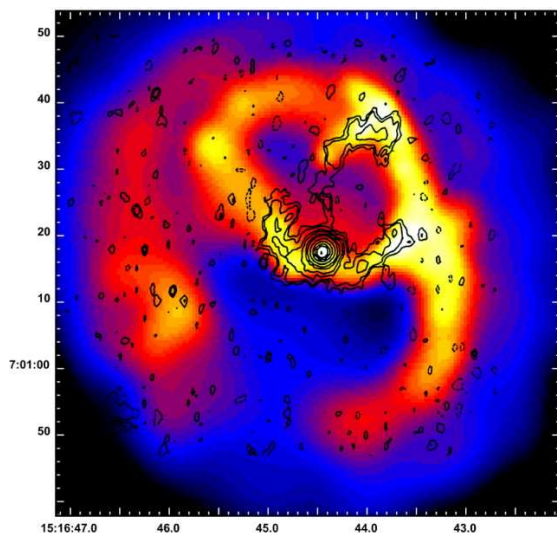


FIG. 7.— Overlay of optical emission line contours from Baum et al. (1988) onto the adaptively-smoothed *Chandra* image of the center of Abell 2052 (Blanton et al. 2001).

emission. Extrapolating the smooth density profile of the cluster outside of the shells into the center of the cluster shows that the mass of gas that would have filled the holes is consistent with the mass of gas currently found in the shells. This confirms the visual impression that the ICM has been swept aside by the radio lobes and compressed into the X-ray-bright shells. The temperature map (Figure 6) reveals that the shells surrounding the radio lobes are cool, and show no evidence of being strongly shocked, with a limit to the Mach number of  $\mathcal{M} < 1.2$ . The cooling time in the shells is  $2.6 \times 10^8$  yr. An overlay of optical emission line contours of  $H\alpha + [N II]$  onto the X-ray image (Figure 7) reveals a striking positive correlation between the brightest parts of the X-ray shells and the optical line emission. The optical emission

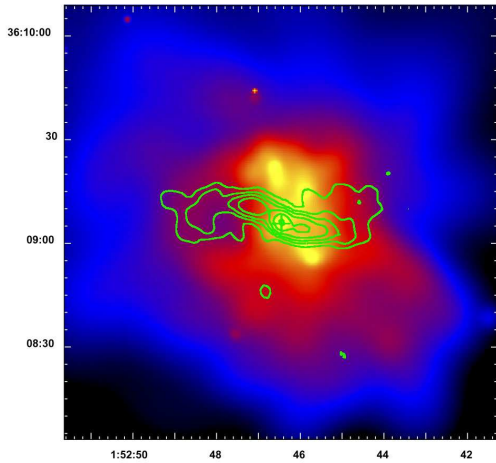


FIG. 8.— Overlay of 1.4 GHz radio contours (Parma et al. 1986) onto the adaptively-smoothed *Chandra* image of Abell 262 (Blanton et al., in preparation).

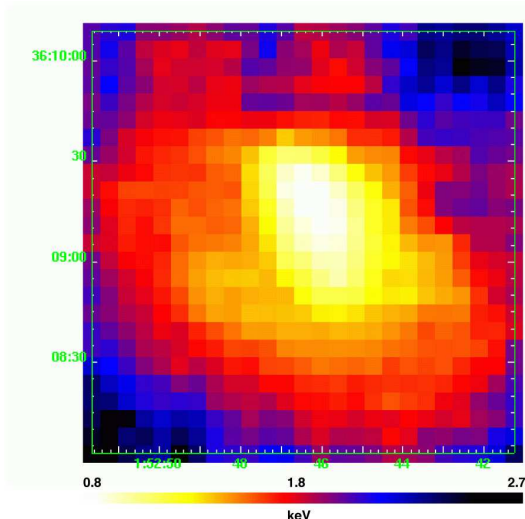


FIG. 9.— Temperature map of the central region of Abell 262 (Blanton et al., in preparation).

represents gas with a temperature of  $\approx 10^4$  K, and the temperature of the X-ray gas in these same regions is  $\approx 10^7$  K, so at least some gas is cooling to low temperatures in this cooling flow cluster. The cooling time of the shells is approximately an order of magnitude longer than the radio source lifetime of  $10^7$  yr, and therefore, the majority of the cooling to low temperatures in the X-ray shells likely occurred when the gas was closer to the cluster center and was subsequently pushed outward by the radio source.

Another example of radio source / X-ray gas interaction in a cooling flow cluster observed with *Chandra* is Abell 262 (Blanton et al., in preparation). This cluster is at a redshift of  $z = 0.0163$  in the same supercluster as Perseus, but is less luminous than Perseus in the X-ray, and has a smaller cooling flow. The double-lobed radio source is orders of magnitude less powerful than those in the previous examples, with a power at 1.4 GHz of only

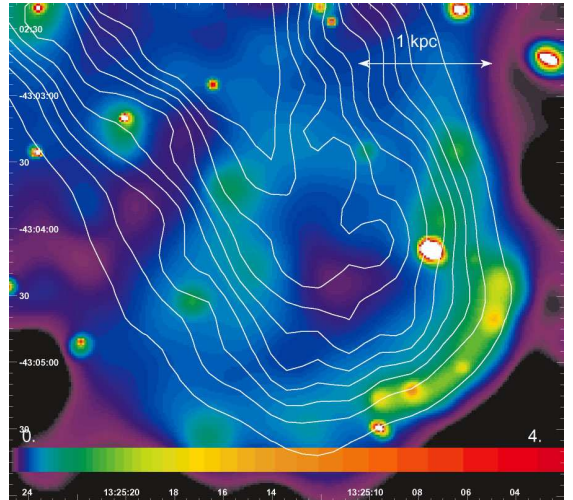


FIG. 10.— Adaptively-smoothed *Chandra* image of the SW lobe of Cen A, with radio contours superposed (Kraft et al. 2003). The bright cap of emission is thought to be ISM that has been shocked by the radio source.

$P_{1.4} = 4.7 \times 10^{22} \text{ W Hz}^{-1}$  (Parma et al. 1986). Still, the radio source has blown a bubble in the ICM, clearly seen to the east of the cluster center (Figure 8). This bubble is much smaller than those in the other clusters discussed above, with a diameter of 5 kpc compared to 20–25 kpc for the others. Similar to the other cases, the cooling time for the gas surrounding the radio lobes is  $3 \times 10^8$  yr, and the temperature map shows no evidence of strong-shock heating (Figure 9).

### 3. Evidence of Shock Heating in Galaxies

As described in the previous section, there is currently no direct evidence for strong-shock heating in cooling flow clusters from the current outburst of the radio source. The temperature maps reveal that the compressed ICM in the shells surrounding the radio bubbles is cool.

It is worth mentioning here examples of what appears to be shock heating of X-ray-emitting gas by a radio source. The first, and more obvious case, is that of the nearby radio galaxy, Centaurus A. This E galaxy was observed with *Chandra* and *XMM-Newton*, as described in Kraft et al. (2003). It is the nearest active galaxy, at a distance of 3.4 Mpc. The radio source is a double-lobed FR I with a power of  $1.9 \times 10^{24} \text{ W Hz}^{-1}$  at 1.4 GHz. There is a shell or cap of emission seen in the X-ray along the edge of the SW radio lobe. This feature was interpreted as shocked interstellar medium (ISM), and exhibits a temperature and pressure that are higher than its surroundings. The pressure jump is consistent with a shock with a Mach number of  $\mathcal{M} = 8.5$ . The brightened cap of emission is shown in Figure 10 (Kraft et al. 2003). While the shocked gas here is ISM, rather than ICM, it still represents the type of signature we might expect to see in cluster gas that has been shocked by a radio source.

Another case is the elliptical galaxy NGC 4636. This galaxy is located in the outer part of the Virgo clus-

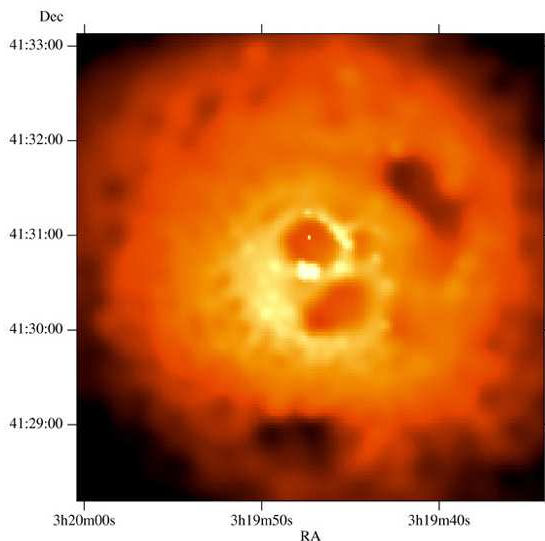


FIG. 11.— Adaptively-smoothed *Chandra* image of the center of the Perseus cluster. The inner bubbles that are associated with the current 1.4 GHz radio emission are seen, as well as two ghost cavities to the S and NW of the cluster center. NASA/IOA/A. Fabian et al.

ter. The *Chandra* image (Jones et al. 2002) shows bright arm-like features with sharp edges. These arm-like features have higher temperatures and pressures than the surrounding gas, consistent with gas that experienced a shock with Mach number  $\mathcal{M} = 1.73$ . However, there is no strong radio source that currently corresponds with the arm-like features, and they may or may not result from a previous radio outburst.

#### 4. Pressure in X-ray Shells

A common feature of the X-ray-bright shells surrounding the radio bubbles shown in §2 is that the pressure measured for the shells is approximately equal to that just outside of them. In other words, there is no evidence for a strong shock. Another feature common to many of these objects is that the pressure measured in the X-ray-bright shells is about an order of magnitude higher than the pressure measured from the radio data within the radio-bright bubbles, assuming equipartition of energies (an example is Abell 2052, with an X-ray shell pressure of  $1.5 \times 10^{-10}$  dyn cm $^{-2}$  [Blanton et al. 2001], and a radio equipartition pressure of  $2 \times 10^{-11}$  dyn cm $^{-2}$  [Zhao et al. 1993]). However, we expect that the bubbles and the shells are in pressure equilibrium, since otherwise they would collapse and fill in. Therefore, either some of the assumptions made for the equipartition pressure estimates are incorrect, or there is an additional source of pressure within the radio bubbles. This additional pressure component may be magnetic fields, low energy relativistic electrons, or very hot, diffuse, thermal gas that would not be detected by *Chandra* because of its low surface brightness in the *Chandra* energy band. The temperature of hot, thermal gas that would provide the required pressure to support the X-ray shells has been limited to  $> 15$  keV for Hydra A (Nulsen et al. 2002),  $> 11$  keV for Perseus (Schmidt et al. 2002), and  $> 20$

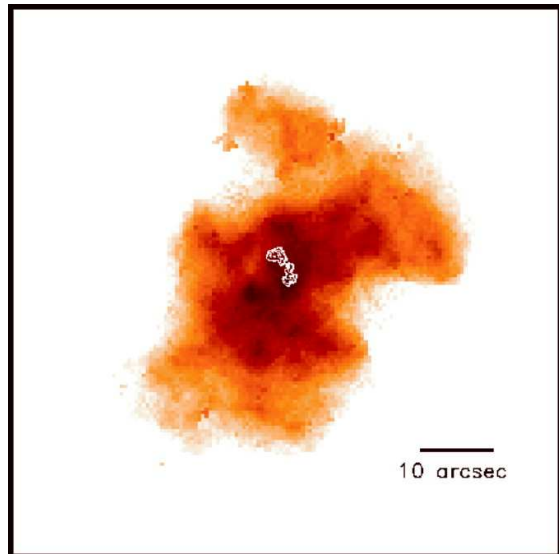


FIG. 12.— The central region of Abell 2597 as observed by *Chandra*, after subtracting a smooth background cluster model. The contours of the small central radio source are superposed. Outer ghost cavities are to the NE and SW of the cluster center and are not clearly associated with the 8.44 GHz radio contours shown here. This figure is from McNamara et al. (2001).

keV for Abell 2052 (Blanton et al. 2003). High sensitivity at high energies is necessary to detect diffuse gas at such temperatures, and *XMM-Newton* or the upcoming *Constellation-X* may be able to detect it.

A detection of gas within an X-ray depression with a temperature significantly hotter than its surroundings has been made using *Chandra* data of the cooling flow cluster MKW 3s (Mazzotta et al. 2002). The gas in the bubble is hotter than the gas at any radius in the cluster, and the temperature measurement is therefore not a projection effect. The deprojected gas temperature within the bubble is 7.5 keV, compared with a temperature of 3.5–4 keV for the surrounding emission. This cluster contains a central radio source, however the 1.4 GHz radio emission is not directly connected with the X-ray depression, as shown in Mazzotta et al. (2002).

#### 5. Buoyantly Rising Bubbles

The density inside the radio bubbles is much lower than that of the ambient gas, so the bubbles should be buoyant and rise outward in the clusters. These rising bubbles can transport energy and magnetic fields into the clusters.

Evidence of bubbles that have risen buoyantly away from the cluster centers has been found in the Perseus (Fabian et al. 2000) and Abell 2597 (McNamara et al. 2001) clusters. These bubbles are not spatially coincident with the 1.4 GHz (Perseus) or 8.44 GHz (Abell 2597) radio contours from the central AGN, and are farther from the cluster center than the radio emission. These features have been referred to as “ghost bubbles” or “ghost cavities” and are thought to result from a previous outburst of the radio source. Examples of these features are shown in Figures 11 (Perseus, Fabian et al. 2000) and 12 (Abell 2597, McNamara et al. 2001). The buoyancy rise time for the ghost cavities to arrive at their projected positions

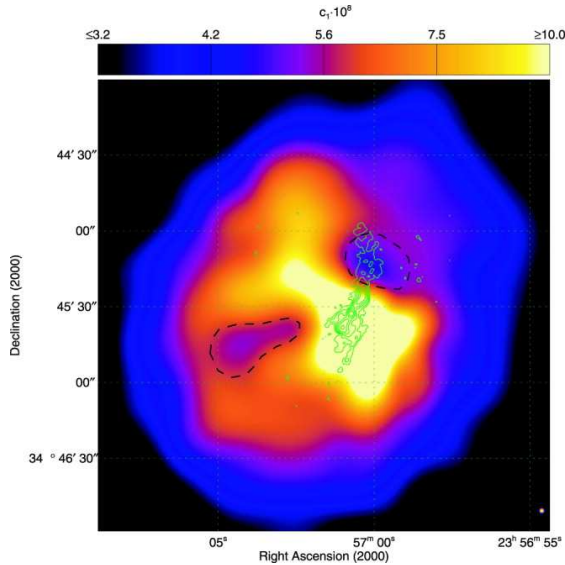


FIG. 13.— Adaptively-smoothed *Chandra* image of the cooling flow cluster Abell 4059. Contours of the 8 GHz radio emission are superposed. The radio emission only partly fills the cavities in the X-ray (Heinz et al. 2002).

has been calculated for these objects, and this timescale reveals the repetition rate of the radio outbursts from the AGN, assuming that the cavities result from a previous outburst. For A2597, for example, the repetition rate is approximately  $10^8$  yr. This is similar to the cooling time of the central gas, suggesting that a feedback process is operating, where cooling gas fuels the AGN, the AGN has an outburst and heats the gas, then the gas cools and fuels the AGN, etc. (McNamara et al. 2001).

Further evidence that the ghost cavities were created by radio lobes earlier in the life of the AGN comes from the detection of low frequency radio emission that is spatially coincident with the outer cavities. The clearest example of this correlation is found in the Perseus cluster when the 74 MHz radio emission is compared with the X-ray emission (Fabian et al. 2002). There also appears to be a similar correlation in the Abell 2597 cluster, based on the comparison of lower frequency radio data than that shown in Fig. 12 and the *Chandra* image (McNamara et al. 2001).

## 6. Intermediate Cases

In the example cooling flow clusters with central radio sources described above, there is either a clear correlation between the radio data and the X-ray emission, such that the radio emission fills the bubbles in the X-ray, or the bubbles are completely devoid of (high frequency) radio emission (the ghost cavities). In addition to these examples, there also exist intermediate cases, “missing links” as suggested by Heinz et al. 2002, where the radio emission partly fills the holes seen in the X-ray. In these cases, it is possible that the radio emission that previously filled the cavities has faded, due to synchrotron losses of the relativistic electrons. Good examples of these intermediate cases are Abell 4059 (Figure 13, Heinz et al. 2002) and Abell 478 (Figure 14, Sun et al. 2003).

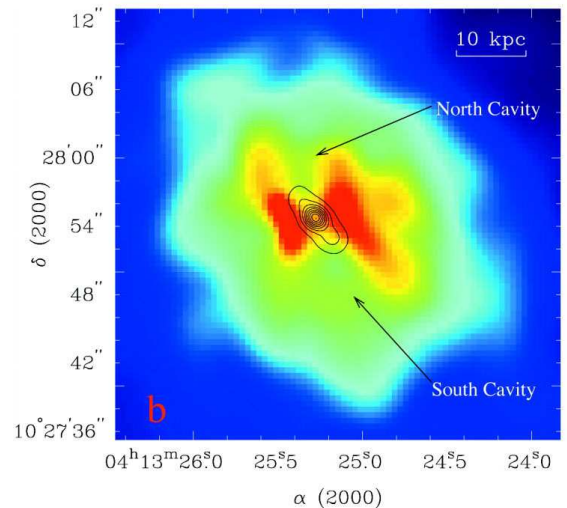


FIG. 14.— Adaptively-smoothed *Chandra* image of the cooling flow cluster Abell 478, with contours of the 1.4 GHz radio emission overlaid. This is a similar case to that of Abell 4059, where the radio emission only partly fills the X-ray holes (Sun et al. 2003).

## 7. Entrainment of Cool Gas

Buoyantly rising bubbles transport energy and magnetic fields outward into clusters. In addition, these rising bubbles create channels in the ICM, and entrain cool cluster gas from the center outward, where it will be mixed with hotter gas.

This type of entrainment is seen clearly in M87 in the Virgo cluster (Young et al. 2002). In this system, the X-ray temperature map reveals that an arc of cool gas follows the same path as the radio lobes. The metallicity in the arc is somewhat higher than the surroundings, which is consistent with the picture of the gas in the arc originating closer to the cluster center, where the average metallicity is higher than in the outer regions of the cluster.

An additional example is Abell 133 (Fujita et al. 2002). This cluster includes a radio source that is offset from the center of the cluster. The radio source was originally thought to be a radio relic, likely produced from a merger shock. The *Chandra* image revealed a filament connecting the radio source with the cluster center. The filament is cool, and shows no evidence of shocks. Fujita et al. surmise that the radio emission is probably a detached lobe from the central AGN. The lobe may have been displaced by the motion of the cD or through buoyancy. The filament of X-ray emission is likely to be cool gas that was entrained outward from the center of the cluster by the radio source.

## 8. Can Radio Sources Offset the Cooling in Cooling Flows?

We have seen that radio sources have a profound effect on the X-ray-emitting ICM, inflating bubbles that rise buoyantly in the clusters. But is the energy deposition into the ICM from the radio sources sufficient to account for the lack of gas seen at very low temperatures in cooling flow clusters? Using the pressures of the X-ray-

bright shells surrounding the bubbles and the volumes of the bubbles, we can determine the total energy output of a radio source. The energy output includes both the internal energy of the bubble and the work done to expand the bubble. From Churazov et al. (2002), the total energy required for a radio source to inflate a bubble in the ICM is

$$E_{\text{rad}} = \frac{1}{(\gamma - 1)}PV + PdV = \frac{\gamma}{(\gamma - 1)}PV, \quad (1)$$

where  $V$  is the volume of the bubble, and  $\gamma$  is the mean adiabatic index of the fluid in the bubble ( $5/3$  for non-relativistic gas or  $4/3$  for relativistic gas). To get the average rate of energy input from a central radio source, we divide this energy by the repetition rate of the radio source, based on the buoyancy rise time of ghost cavities, and with a value of approximately  $10^8$  yr (see §5). We compare this energy input rate with the luminosity of cooling gas derived from spectral fitting to the X-ray data. The luminosity of isobaric cooling gas is given by

$$L_{\text{cool}} = \frac{5}{2} \frac{kT}{\mu m_p} \dot{M}, \quad (2)$$

where  $kT$  is the temperature of the ICM outside of the cooling region,  $\dot{M}$  is the mass deposition rate, and  $\mu$  is the mean mass per particle in units of the proton mass.

For the case of Hydra A (McNamara et al. 2000; David et al. 2001; Nulsen et al. 2002), the total power output of the radio source, derived as described above from the X-ray pressure and volumes of the radio cavities, is  $2.7 \times 10^{44}$  erg s $^{-1}$ . The cooling luminosity, using  $\dot{M} = 300 M_{\odot}$  yr $^{-1}$  and  $kT = 3.4$  keV, is  $L_{\text{cool}} = 3 \times 10^{44}$  erg s $^{-1}$ . Therefore, in this case, just based on these simple energy arguments, the radio source is depositing enough energy into the ICM on average to offset the cooling gas. A similar test performed for Abell 2052 (Blanton et al. 2003) shows that the radio source also has sufficient power ( $3 \times 10^{43}$  erg s $^{-1}$ ) to offset the cooling gas ( $L_{\text{cool}} = 3 \times 10^{43}$  erg s $^{-1}$  with  $\dot{M} = 42 M_{\odot}$  yr $^{-1}$  and  $kT = 3$  keV). The situation is different for Abell 262 (Blanton et al., in preparation), where the radio source power ( $3.4 \times 10^{41}$  erg s $^{-1}$ ) falls more than an order of magnitude short of that required to offset the cooling luminosity ( $L_{\text{cool}} = 1.3 \times 10^{43}$  erg s $^{-1}$ , using  $kT = 2.65$  keV, and the mass-deposition rate of  $18.8 M_{\odot}$  yr $^{-1}$ ). However, this radio source is much less luminous than Hydra A or 3C 317 in Abell 2052, and the bubble volume inflated in Abell 262 is much smaller than that in the others. The bubble diameter is only 5 kpc in Abell 262 compared to diameters of 20 – 25 kpc for the others.

Since we are assuming that the power output from the radio source is an average over many outbursts of the AGN, it may be that a previous outburst of the radio source in Abell 262 was much more powerful, so that, on average, the cooling could still be balanced by the input of energy from the radio source.

## 9. Conclusions

Central radio-emitting AGN strongly affect the X-ray-emitting gas in cooling flows. The radio sources create cavities or “bubbles” in the X-ray gas, which, in turn, confines the radio sources. In all clusters observed so far, there is no evidence that the radio sources are strongly shocking the ICM. The X-ray-bright shells surrounding the bubbles are cool, not hot. Weak shocks may have occurred in the past, creating the dense shells. The only evidence for strong-shock heating of a similar nature has been seen in radio-ISM interactions in galaxies, and there are only very few cases of this so far.

The X-ray pressures derived from the shells surrounding the bubbles are approximately ten times higher than the radio equipartition pressures. There may be problems with some of the equipartition assumptions or additional contributions to the pressure within the radio bubbles. One possibility for this additional pressure source is very hot, diffuse, thermal gas.

The bubble interiors are less dense than their surroundings and therefore will rise buoyantly outward into the clusters. Ghost cavities provide evidence that this process has occurred. The buoyantly-rising bubbles transport energy and magnetic fields into the clusters and they can also entrain cool gas from the cluster centers outward.

The shell pressures and bubble volumes measured in the X-ray can be used to determine the total energy output of the radio sources. A radio source repetition rate of  $\approx 10^8$  yr is derived from the buoyancy rise time of the ghost cavities. A rough comparison of the average energy output of radio sources and the luminosity of cooling gas shows that the radio sources can supply enough energy to offset the cooling in cooling flows, at least in some cases.

I am very grateful to my collaborators, Craig Sarazin, Brian McNamara, Noam Soker, Tracy Clarke, and Mike Wise. Support for E. L. B. was provided by NASA through the *Chandra* Fellowship Program, grant award number PF1-20017, under NASA contract number NAS8-39073.

## References

- Baum, S. A., Heckman, T. M., Bridle, A., van Breugel, W. J. M., & Miley, G. K. 1988, ApJS, 68, 643
- Blanton, E. L., Sarazin, C. L., McNamara, B. R., & Wise, M. W. 2001, ApJ, 558, L15
- Blanton, E. L., Sarazin, C. L., & McNamara, B. R. 2003, ApJ, 585, 227
- Böhringer, H., Voges, W., Fabian, A. C., Edge, A. C., Neumann, D. M. 1993, MNRAS, 264, L25
- Böhringer, H., Matsushita, K., Churazov, E., Ikebe, Y., & Chen, Y. 2002, A&A, 382, 804
- Brüggen, M. 2003, ApJ, 592, 839
- Churazov, E., Sunyaev, R., Forman, W., & Böhringer, H. 2002, MNRAS, 332, 729
- David, L. P., Nulsen, P. E. J., McNamara, B. R., Forman, W., Jones, C., Ponman, T., Robertson, B., & Wise, M. 2001, ApJ, 557, 546
- Dupke, R., & White, R. E. III 2001, High Energy Universe at Sharp Focus: Chandra Science, ed. E. M. Schlegel & S. Vrtillek (San Francisco: ASP Conference Series), 51
- Fabian, A. C., Sanders, J. S., Ettori, S., Taylor, G. B., Allen, S. W., Crawford, C. S., Iwasawa, K., Johnstone, R. M., & Ogle, P. M. 2000, MNRAS, 318, L65

- Fabian, A. C., Mushotzky, R. F., Nulsen, P. E. J., & Peterson, J. R. 2001, *MNRAS*, 321, L20
- Fabian, A. C., Celotti, A., Blundell, K. M., Kassim, N. E., & Perley, R. A. 2002, *MNRAS*, 331, 369
- Fabian, A. C., Sanders, J. S., Allen, S. W., Crawford, C. S., Iwasawa, K., Johnstone, R. M., Schmidt, R. W., & Taylor, G. B. 2003, *MNRAS*, 344, L43
- Fujita, Y., Sarazin, C. L., Kempner, J. C., Rudnick, L., Slee, O. B., Roy, A. L., Andernach, H., & Ehle, M. 2002, *ApJ*, 575, 764
- Heinz, S., Reynolds, C. S., & Begelman, M. C. 1998, *ApJ*, 501, 126
- Heinz, S., Choi, Y.-Y., Reynolds, C. S., & Begelman, M. C. 2002, *ApJ*, 569, L79
- Huang, Z., & Sarazin, C. L. 1998, *ApJ*, 496, 728
- Johnstone, R. M., Allen, S. W., Fabian, A. C., & Sanders, J. S. 2002, *MNRAS*, 336, 299
- Jones, C., Forman, W., Vikhlinin, A., Markevitch, M., David, L. P., Warmflash, A., Murray, S., & Nulsen, P. E. J. 2002, *ApJ*, 567, L115
- Kaiser, C. R. & Binney, J. 2003, *MNRAS*, 338, 837
- Kraft, R. P., Vázquez, S. E., Forman, W. R., Jones, C., Murray, S. S., Hardcastle, M. J., Worrall, D. M., & Churazov, E. 2003, *ApJ*, 592, 129
- Mazzotta, P., Kaastra, J. S., Paerels, F. B., Ferrigno, C., Colafrancesco, S., Mewe, R., & Forman, W. R. 2002, *ApJ*, 567, L37
- McNamara, B. R., Wise, M., Nulsen, P. E. J., David, L. P., Sarazin, C. L., Bautz, M., Markevitch, M., Vikhlinin, A., Forman, W. R., Jones, C., & Harris, D. E. 2000, *ApJ*, 534, L135
- McNamara, B. R., Wise, M. W., Nulsen, P. E. J., David, L. P., Carilli, C. L., Sarazin, C. L., O'Dea, C. P., Houck, J., Donahue, M., Baum, S., Voit, M., O'Connell, R. W., Koekemoer, A. 2001, *ApJ*, 562, L149
- Nulsen, P. E. J., David, L. P., McNamara, B. R., Jones, C., Forman, W. R., & Wise, M. 2002, *ApJ*, 568, 163
- Parma, P., de Ruiter, H. R., Fanti, C., & Fanti, R. 1986, *A&AS*, 64, 135
- Peterson, J. R., Paerels, F. B. S., Kaastra, J. S., Arnaud, M., Reiprich, T. H., Fabian, A. C., Mushotzky, R. F., Jernigan, J. G., & Sakelliou, I. 2001, *A&A*, 365, L104
- Peterson, J. R., Kahn, S. M., Paerels, F. B. S., Kaastra, J. S., Tamura, T., Bleeker, J. A. M., Ferrigno, C., & Jernigan, J. G. 2003, *ApJ*, 590, 207
- Reynolds, C. S., Heinz, S., & Begelman, M. C. 2002, *MNRAS*, 332, 271
- Rizza, E., Loken, C., Bliton, M., Roettiger, K., Burns, J. O., & Owen, F. N. 2000, *AJ*, 119, 21
- Ruszkowski, M., & Begelman, M. C. 2002, *ApJ*, 581, 223
- Sanders, J. S. & Fabian, A. C. 2002, *MNRAS*, 331, 273
- Schindler, S., Castillo-Morales, A., De Filippis, E., Schwöpe, A., & Wambsganss, J. 2001, *A&A* 376, L27
- Schmidt, R. W., Fabian, A. C., & Sanders, J. S. 2002, *MNRAS*, 337, 71
- Smith, D. A., Wilson, A. S., Arnaud, K. A., Terashima, Y. & Young, A. J. 2002, *ApJ*, 565, 195
- Soker, N., Blanton, E. L., & Sarazin, C. L. 2002, *ApJ*, 573, 533
- Sun, M., Jones, C., Murray, S. S., Allen, S. W., Fabian, A. C., & Edge, A. C. 2003, *ApJ*, 587, 619
- Young, A. J., Wilson, A. S., & Mundell, C. G. 2002, *ApJ*, 579, 560
- Zhao, J.-H., Sumi, D. M., Burns, J. O., & Duric, N. 1993, *ApJ*, 416, 51